

Silicon-on-Insulator Platform for Integrated Wavelength-Selective Components

Dirk Taillaert (1), Roel Baets (1), Pieter Dumon (1), Wim Bogaerts (1), Dries Van Thourhout (1), Bert Luyssaert (1), Vincent Wiaux (2), Stephan Beckx (2), Johan Wouters (2)

1 : Ghent University – IMEC, Department of Information Technology, Sint-Pietersnieuwstraat 41, 9000 Gent, BELGIUM, Email: dirk.taillaert@intec.UGent.be

2 : IMEC v.z.w., Silicon Process Technology Division, Kapeldreef 75, 3001 Leuven, BELGIUM

Abstract— The Silicon-on-Insulator (SOI) platform allows to make ultra-compact photonic integrated circuits by means of standard processes used for silicon CMOS. Basic properties of SOI waveguides and the coupling to fiber are briefly discussed. Afterwards, various WDM-components (filters and demultiplexers) based on high-contrast nanophotonic waveguides in SOI are reported.

I. INTRODUCTION

The implementation of photonic ICs for Wavelength Division Multiplexing (WDM) functions can be done by means of a variety of material systems. For passive functions such as filters and demultiplexers, Silica-based technologies have been very successful to meet the demanding requirements of WDM systems in terms of spectral behaviour (bandwidth, crosstalk...) and losses. However the low refractive index contrast in the Silica system results in large dies, mainly because the waveguide bends have radii in the millimeter range.

In contrast, a Silicon-on-Insulator (SOI) substrate offers the possibility to make waveguides with very high refractive index contrast of the order of 2 to 1 in all directions of confinement. With such strong confinement the typical dimensions of the Silicon core are 200 x 500 nm for single-mode waveguides. These waveguides – often called photonic wires - allow to reduce the bend radius down to a few micrometer. For many types of photonic circuits this means that the die size can be miniaturized by 10-1000 times. The price paid for this dramatic reduction in size is the fact that the tolerances on the dimensions are also reduced. The geometrical precision of the topological layout needs to be of the order of 10 nm or better, so as to achieve a predictable and reproducible effective refractive index as well as to reduce the losses due to roughness.

Electron-beam lithography can meet these stringent requirements and a variety of photonic functions has been demonstrated in SOI by means of this technology [1-4]. One of the major advantages however of SOI-based nanophotonic circuits is the fact that they can be fabricated by means of standard technologies normally used for the industrial manufacturing of microelectronic ICs, such as deep-UV lithography.

In this paper, a variety of wavelength-selective functions implemented in SOI by means of 248 nm deep-UV lithography are discussed. The fabrication technology has been discussed in [5]. This technology has allowed to reproducibly make waveguides with losses of the order of a few dB/cm. In the next section, we briefly discuss the basic waveguides and structures for coupling to fiber. Afterwards the wavelength selective components are presented.

II. SOI WAVEGUIDES

A. Photonic wires

Our structures are made in SOI with a 220 nm thick Si top layer and a 1 μm buried oxide. Pattern definition in resist is done using deep UV (DUV) lithography with an illumination wavelength of 248 nm. The Si layer is then fully etched using a dry etching process. The resulting strip waveguide is drawn in figure 1. The fabrication process is described in detail elsewhere [5]. Optionally, a top cladding such as SiO₂ or polymer can be applied. Resulting waveguides have both a high lateral and vertical refractive index contrast and are also called photonic wires. They are no wider than 600 nm in order to keep them single mode. Earlier, we demonstrated propagation losses as low as 2.4 dB/cm for a 500 nm wide straight wire for TE-like polarisation [6]. These losses are due

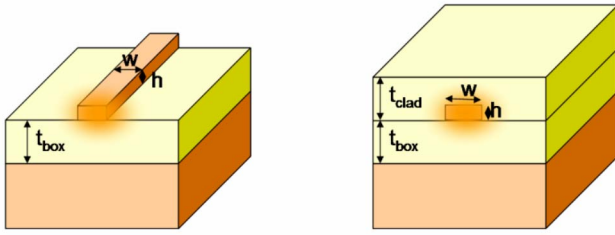


Figure 1 : Basic SOI photonic wire waveguide structure with air top cladding (left) and silica top cladding (right)

to substrate leakage and scattering at sidewall roughness. The propagation losses for TM polarisation are much higher than for TE polarisation. Therefore, in the remainder of the paper only TE polarisation is considered.

It is possible to reduce the polarisation dependency of straight wires by making them more squared [7]. However, obtaining polarisation independent functional circuits is very difficult, if not impossible. A polarisation diversity approach can be used to make polarization independent devices with polarization dependent circuits. Such an approach requires integrated polarization splitters and polarization converters.

B. Coupling to fiber

Coupling light efficiently between a SOI nanophotonic waveguide and an optical fiber is an important issue. Some kind of spot-size converter is needed to adapt the mode of a sub-micrometer sized waveguide to the mode of a single-mode fiber. By using an inverted lateral combined with a fiber-adapted polymer waveguide, a coupling loss below 0.5 dB has already been demonstrated [3,7]. However such a structure requires a taper tip with a width below 100 nm. Because this is very challenging to fabricate using our standard deep-UV lithography, we have used grating couplers as the interface between the integrated circuit and fibers.

An alternative is using grating couplers, consisting of a rather shallow grating, etched in the top silicon layer. Grating couplers are interesting structures for efficient coupling of light into sub-micrometer waveguides. By using a grating coupler, light can be injected anywhere in an optical circuit and not only at the edges. So there is no need to polish facets to couple light in and out. Standard single-mode fiber can be used and also the sensitivity to alignment errors is better compared to edge coupling. The grating coupler couples light to a wide SOI waveguide, this wide waveguide is connected to a photonic wire by a taper structure. This is illustrated in figure 2.

The couplers used to characterize the devices presented in this paper, have a 610 nm period, 50 nm etch depth and 50% duty cycle [6]. The transmission spectrum is approximately Gaussian with a maximum transmission efficiency of 20% and a 3dB bandwidth of 60 nm. It should be noted that this

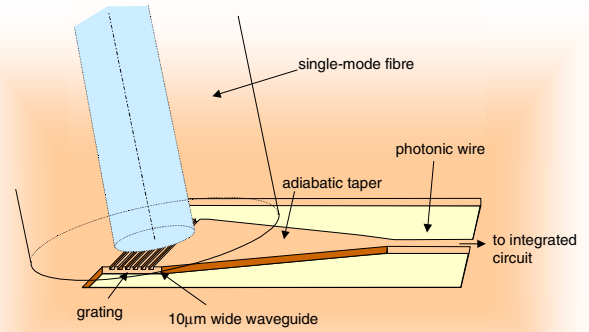


Figure 2 : Grating coupler for coupling between a SOI photonic wire and an optical fiber.

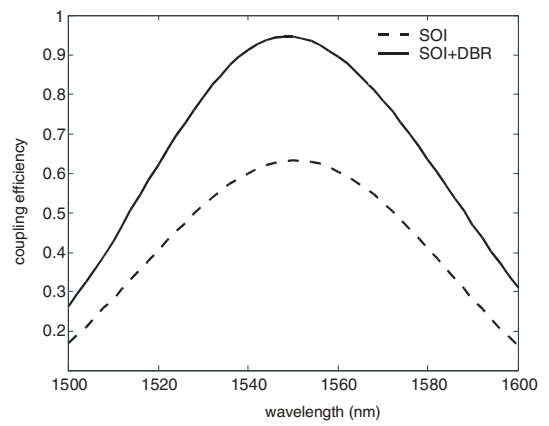


Figure 3 : Calculated coupling efficiency to fiber of an optimized grating coupler [8].

efficiency can be improved dramatically by using more optimized grating couplers. We have already measured 33% on improved grating couplers. A further enhancement is the use of non-uniform gratings and an optimized layer structure. In [8], we have presented simulation results on these optimized grating couplers. The resulting efficiency versus wavelength is shown in figure 3. It is possible to achieve more than 90% efficiency when using SOI with an additional mirror [9] under the waveguide. For standard SOI, the efficiency is limited to approximately 60%.

These grating couplers are also polarization selective. However, by extending the principle of the fiber coupling gratings to 2-D gratings, a polarization splitter coupler can be made [10] that couples light from the fiber to the fundamental TE mode of two waveguides. That coupler can be used in a polarisation diversity configuration. However, more work is needed to improve the efficiency of those couplers.

III. RING RESONATORS

Microring resonators in SOI can be a building block for densely integrated wavelength selective filters, which can be used for WDM purposes and other applications. The SOI material system used here has both a very high lateral and vertical index contrast. This enables fabrication of bend waveguides with radii down to a few microns with low radiation loss. This in turn allows for very large free spectral ranges (FSR) which is important for the fabrication of add-drop filters. A large finesse and high extinction ratios are important too. To achieve good add-drop filters, the line shape of the microring still needs to be altered. This can be done by using higher-order filters consisting of multiple rings in series. However, the study of single ring filters is a first step towards this goal.

Reliable fabrication of such devices is challenging however. In most cases, electron-beam lithography is used to define patterns in a resist. We present microring resonators in SOI photonic wires fabricated using CMOS fabrication technology. These wires are strip-like waveguides with submicron dimensions. The resonators have radii up to $8\ \mu\text{m}$ and are laterally coupled to two waveguides for coupling in and out the resonator. We studied different coupling alternatives in order to achieve low crosstalk and high finesse while maintaining a large free spectral range.

A. Circular ring resonators

The first devices fabricated are circular ring resonators coupled to two straight waveguides. The gap between the ring and the straight waveguide is limited to approximately $200\ \text{nm}$ due to technological limitations. This makes coupling between the ring and waveguides difficult. In Figure 4, the power coupling coefficient is shown for different gap widths for a $5\ \mu\text{m}$ radius ring. These are the results of simulations based on coupled mode theory [11]. The coupling coefficient can be increased by adding a top cladding with a higher refractive index.

With a $5\ \mu\text{m}$ radius ring, a FSR of $17\ \text{nm}$ is obtained but the drop efficiency is very low due to the low coupling. We applied a BCB top cladding in order to enhance the coupling. The BCB polymer has a slightly higher refractive index (1.5) than the air cladding. The increase in the coupling coefficient is clear from simulations (figure 4). Reduced waveguide dispersion also leads to a net increase of the FSR to $18.5\ \text{nm}$. The transmission spectra are shown in figure 5. This is the fiber to fiber transmission and includes the losses of input and output couplers. Due to the low coupling coefficient and the high FSR, the finesse of this kind of ring resonator is high, up to 120. However, for WDM purposes coupling should be increased. Therefore, we looked at other ring resonator configurations to enhance coupling between the cavity and the waveguides.

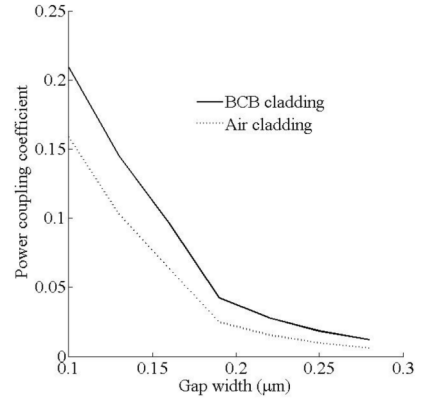


Figure 4: Simulation of the power coupling coefficient versus gap width between ring and straight waveguide.

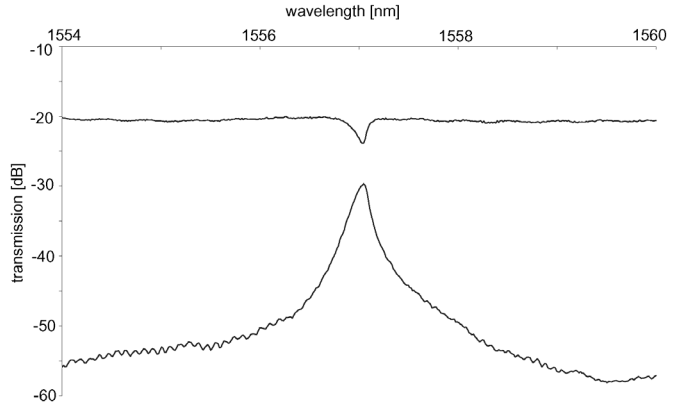


Figure 5: Detail of transmission spectra of a ring resonator with $5\ \mu\text{m}$ radius with a BCB top cladding

B. Racetrack resonators

One option is to include a straight coupling section, leading to a racetrack form resonator (Fig. 6). We have fabricated racetracks with radii of the bend section between 1 and $6\ \mu\text{m}$. Transmission spectra of a racetrack with $1\ \mu\text{m}$ radius are shown in Fig. 6. With a $1\ \mu\text{m}$ radius, a Q of around 2100 is obtained and the FSR is larger than $40\ \text{nm}$, but the drop efficiency is low. For larger radii, the ring losses decrease quickly. With a $2\ \mu\text{m}$ radius, the drop efficiency is already much larger and Q factors in the range 5000-9000 are obtained. We have also fabricated racetracks with $5\ \mu\text{m}$ radius and larger coupling section [12]. The larger coupling leads to a high add-drop extinction ratio of $-20\ \text{dB}$ and 50-70% drop efficiency at Q factors still larger than 3000. This is illustrated in Fig. 7. Due to the larger resonator, the FSR is reduced to approximately $12\ \text{nm}$.

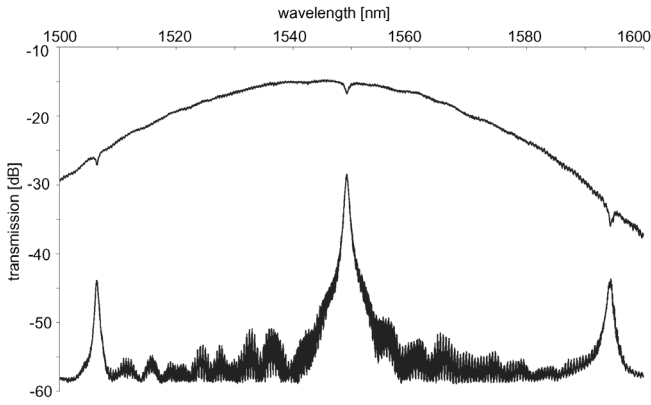
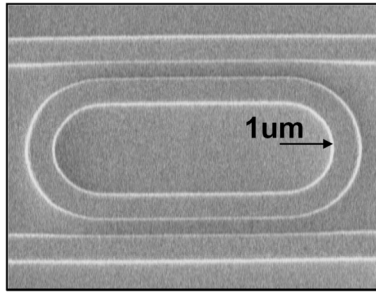


Figure 6 : Racetrack with 1 μm bend radius, SEM picture (top) and transmission spectra (bottom)

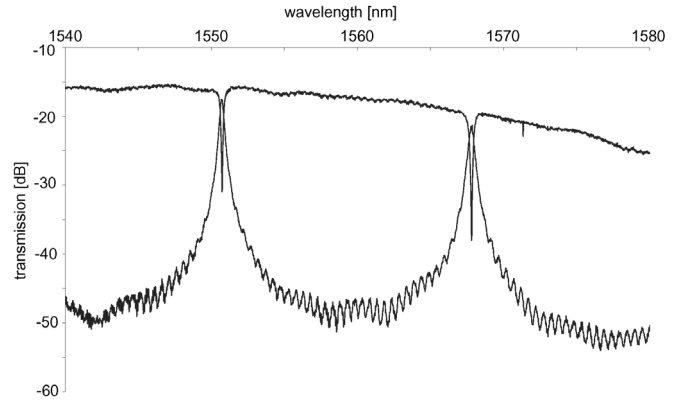
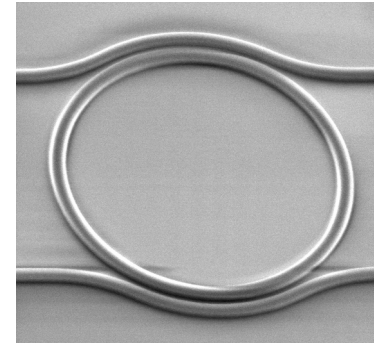


Figure 8: SEM picture and transmission spectra of a bend-coupled ring resonator with 5 μm radius

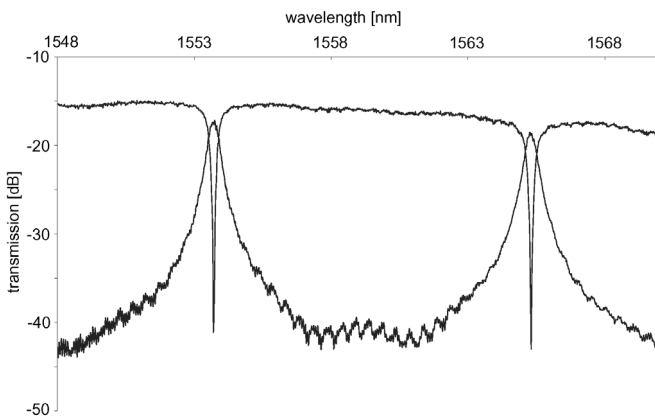


Figure 7 : Pass and drop transmission spectra of a racetrack resonator with a bend radius of 5 μm and a coupling section length of 3 μm .

C. Ring resonators coupled to bend waveguides.

While racetrack resonators can clearly enhance coupling, their FSR is limited. Another option is coupling to bend waveguides [13]. The topology is illustrated by Fig. 8. By carefully choosing the widths of cavity and bus waveguides, a good phase matching can be obtained and coupling can be high without lowering the FSR as in the case of the racetrack resonator. We fabricated bend-coupled resonators with 5 μm and 8 μm radius. The amount of coupling is varied by varying the angle over which both waveguides are coupled. Coupling is large enough to obtain a relatively high extinction ratio (-10 to -15dB) and high drop efficiency, although these first devices not optimized yet.

The dimensions of these ring resonators are critical. The gap of the directional coupler is typically 200-250 nm wide and the coupling strength depends strongly on this value. The width of the waveguide in the ring has a strong influence on the resonance wavelength: a width change of 5 nm leads to a shift of about 15 nm. This sensitivity calls for a thorough optimisation of the design and fabrication process including line bias effects and proximity corrections.

D. First order demultiplexer

We have fabricated a 4 channel add-drop filter with racetrack resonators with different radius [14]. By varying the radius, the resonance wavelength is changed and each cavity is tuned to another set of dropped wavelengths. One must keep in mind that with this approach the FSR also varies. Figure 9 shows the overlaid transmission spectra for 4 resonators with bend radius 6, 6.02, 6.04 and 6.08 μm . A BCB top cladding was applied. We see that a large part of the FSR can be reached by changing the radius over only 80 nm. However, the resonance wavelength doesn't increase linearly with the radius. This is partly due the discretisation on the mask, but other configurations will be studied to avoid this problem and achieve better control of the wavelength spacing.

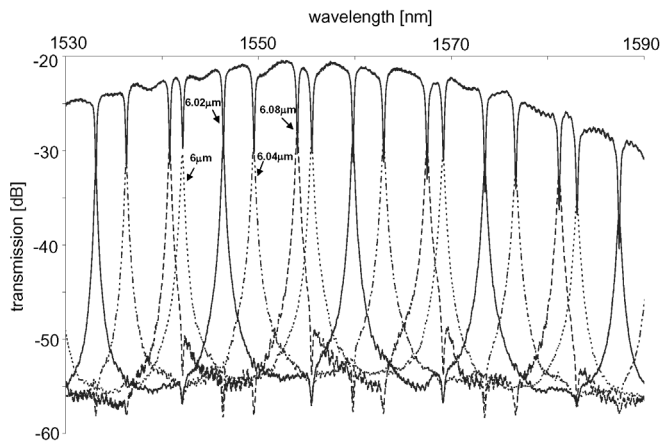


Figure 9: Overlaid transmission spectra of a 1-by-4 demux with 4 racetrack resonators with varying bend radius (indicated)

IV. ARRAYED WAVEGUIDE GRATINGS

Generally arrayed waveguide grating (AWG) devices can serve as multiplexers, demultiplexers, filters and add-drop devices in WDM applications. Currently, Silica-on-silicon AWGs are commercially available devices and have a footprint of several cm^2 .

We have designed and fabricated an 8-channel AWG in SOI. The device, shown in figure 10, has a footprint of $380 \mu\text{m} \times 290 \mu\text{m}$, or about 0.1mm^2 . The on-chip insertion loss is approximately 8 dB. The channel spacing is 3 nm, with a free spectral range of 24 nm. However, the crosstalk is still significant, between 6 dB and 9 dB [15]. The transfer from an input port to the 8 output waveguides is also plotted in Figure 10. We believe the insertion loss is mainly caused by reflections in the star coupler and can be reduced by adapting the transition zone between the grating arms and the star coupler.

The main problem however is the high crosstalk level, limited to values around -7dB , which is clearly not sufficient for practical applications. Also in [1] an AWG fabricated using SOI-wires was presented. The authors optimized the devices for compactness and demonstrated a $110 \times 93 \mu\text{m}^2$ device with a 6 nm channel spacing and a 90 nm FSR. However, also in this case, the crosstalk was limited to a few dB.

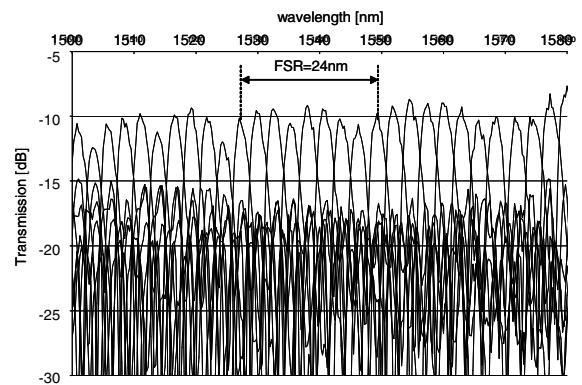
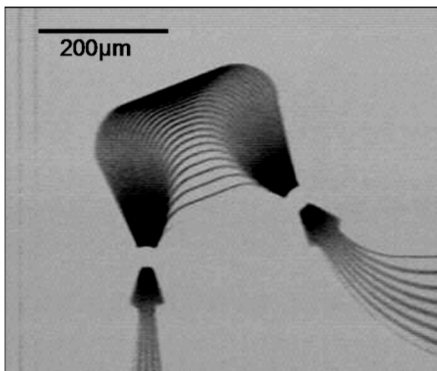


Fig. 10 Microscope image of the 8-channel AWG and superimposed plot of the 8 transmission spectra.

The high crosstalk may be caused by several reasons such as reflections or overspill in the star coupler. We believe the crosstalk is mainly caused by phase errors in the grating arms however. Due to the high refractive index contrast even the very small roughness can lead to random phase fluctuations over the array arms and lead to the observed crosstalk level.

V. CASCADED MACH-ZEHNDER (CMZ) FILTERS

SOI-wire based Cascaded Mach-Zehnder interferometers have been demonstrated by several authors [16,17]. As shown in figure 11, such filters consist of a series of Mach-Zehnder interferometers with constant path-length difference but with varying coupling ratio. The coupling ratios are optimized to obtain the desired wavelength dependent transmittance. A CMZ filter can be designed for Chebyshev-type filter behaviour with low sidelobe levels.

Figure 11 shows an example of a 5-stage CMZ, consisting of 6 directional couplers and 5 delay sections. The isolated waveguides have a width of 565 nm while the waveguides in the coupling sections are only 535 nm wide due to optical proximity effects. The gap width itself is 220 nm. Figure 12 shows the transmission characteristic of this component in both the pass and the drop port, normalized to the transmission of a simple straight waveguide. We can see a well-defined filter characteristic with a bandwidth of 2.6 nm, a free spectral range of 17 nm and a coupling efficiency of

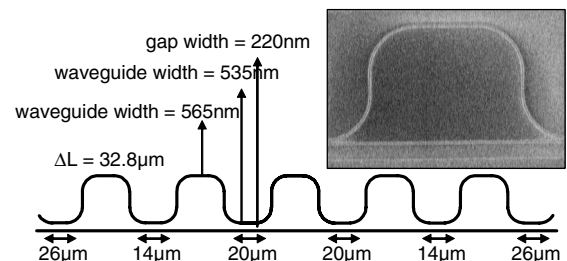


Fig. 11 Design of a 5-stage CMZ filter.

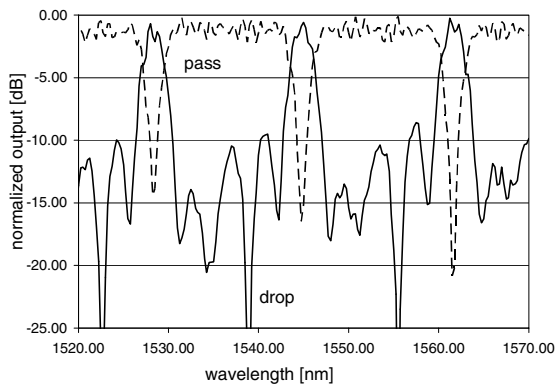


Fig. 12 Transmission characteristic of the five-stage CMZ from figure 11.

almost 100%. The crosstalk of 10 dB is still relatively high and caused by a non optimized choice of the coupling ratios and by phase errors in the interferometers.

In [16], a similar device having a -12 dB crosstalk level and a 80 nm spectral range was demonstrated. By cascading three devices in series, the crosstalk could be increased to -30 dB. Also multiple wavelength add-drops were demonstrated.

VI. CONCLUSIONS

The results shown here demonstrate that a variety of passive WDM-functions can be implemented on SOI by means of CMOS-compatible processes. While the performance of these first devices is promising, there is certainly a lot of room for improvement by refining the designs and optimising the technology. This should result in predictable control of geometry at the nanometer level, as needed for these nanophotonic circuits.

ACKNOWLEDGMENTS

Part of this work was supported by the European Union through the IST-PICCO and IST-PICMOS project and by the Belgian IAP-PHOTON network project. P. Dumon and B. Luyssaert thank the Flemish Institute for the industrial advancement of scientific and technological Research (IWT) for a specialization grant. W. Bogaerts acknowledges the Flemish Fund for Scientific Research (FWO).

The authors would also like to thank D. Vangoidsenhoven, Rudi de Ruyter and Johan Mees.

REFERENCES

- [1] T. Fukazawa, F. Ohno and T. Baba, "Very compact arrayed-waveguide-grating demultiplexer using Si photonic wire waveguides," *Japanese Journal of Applied Physics*, Vol. 43, No. 5B, pp. L 673–L 675, 2004
- [2] B. Little, J. Foresi, G. Steinmeyer, E. Thoen, S. Chu, H. Haus, E. Ippen, L. Kimerling, and W. Greene, "Ultra-compact Si-SiO₂ microring resonator optical channel dropping filters," *IEEE Phot. Technol. Lett.*, vol. 10, no. 4, pp. 549–551, 1998
- [3] S. J. McNab, N. Moll, and Y. Vlasov, "Ultra-low loss photonic integrated circuit with membrane-type photonic crystal waveguides," *Opt. Express*, vol. 11, no. 22, pp. 2927–2939, Nov. 2003.
- [4] M. Notomi, A. Shinya, S. Mitsugi, E. Kuramochi, and H. -Y. Ryu, "Waveguides, resonators and their coupled elements in photonic crystal slabs," *Opt. Express*, vol. 12, no. 8, pp. 1551–1561, April 2004.
- [5] W. Bogaerts, R. Baets, P. Dumon, V. Wiaux, S. Beckx, D. Taillaert, B. Luyssaert, J. Van Campenhout, P. Bienstman, D. Van Thourhout, "Nanophotonic Waveguides in Silicon-on-Insulator Fabricated with CMOS Technology," *IEEE J. Lightwave Technol.*, vol. 23, pp. 401–412, 2005
- [6] W. Bogaerts, D. Taillaert, B. Luyssaert, P. Dumon, J. Van Campenhout, P. Bienstman, D. Van Thourhout, R. Baets, V. Wiaux, S. Beckx, "Basic structures for photonic integrated circuits in Silicon-on-insulator," *Opt. Express*, vol. 12, no. 8, pp. 1583–1591, April 2004.
- [7] T. Shoji, T. Tsuchizawa, T. Watanabe, K. Yamada, and H. Morita, "Low loss mode size converter from 0.3 μ m square Si wire waveguides to single-mode fibres," *Electron. Lett.*, vol. 38, pp. 1669–1670, 2002
- [8] D. Taillaert, P. Bienstman, R. Baets, "Compact efficient broadband grating coupler for silicon-on-insulator waveguides," *Optics Letters*, vol. 29, pp. 2749–2751, 2004.
- [9] M. Emsley, O. Dosunmu, and M. Unlu, "Silicon substrates with buried distributed Bragg reflectors for resonant cavity-enhanced optoelectronics," *IEEE J. Select. Topics Quantum Electron.*, vol. 8, pp. 948–955, 2002.
- [10] D. Taillaert, H. Chong, P. Borel, L. Frandsen, R. De La Rue, and R. Baets, "A compact two-dimensional grating coupler used as a polarization splitter," *IEEE Photon. Technol. Lett.*, vol. 15, pp. 1249–1251, 2003.
- [11] R. Stoffer et al., "Comparison of coupled mode theory and FDTD simulations of coupling between bent and straight optical waveguides", *International school of Quantum Electronics*, 39th course, Erice, Italy, October 2003, pp. 366–377
- [12] P. Dumon, W. Bogaerts, V. Wiaux, J. Wouters, S. Beckx, J. Van Campenhout, D. Taillaert, B. Luyssaert, P. Bienstman, D. Van Thourhout, R. Baets, "Low-loss SOI photonic wires and ring resonators fabricated with deep UV lithography," *IEEE Photon. Tech. Lett.*, vol. 16, pp. 1328–1330, 2004
- [13] M.K. Chin and S.T. Ho, "Design and Modeling of Waveguide-Coupled Single-Mode Microring Resonators", *IEEE J. Lightwave Technol.*, vol. 16(8), pp. 1433–1446, 1998
- [14] P. Dumon, I. Christiaens, W. Bogaerts, Vincent Wiaux, Johan Wouters, Stephan Beckx, D. Van Thourhout, R. Baets, "Microring resonators in Silicon-on-Insulator", 12th European Conference on Integrated Optics, p. ThA2-6, Grenoble, France, April 2005
- [15] P. Dumon, W. Bogaerts, D. Van Thourhout, D. Taillaert, V. Wiaux, S. Beckx, J. Wouters, R. Baets, "Wavelength-selective components in SOI photonic wires fabricated with deep UV lithography," 1st Int. Conf on Group IV Photonics, p. WB 5, Hongkong, Sept 2004
- [16] K. Yamada, T. Shoji, T. Tsuchizawa, T. Watanabe, J. Takahashi, S. Itabashi, "Silicon-wire-based ultrasmall lattice filters with wide free spectral ranges", *Optics Letters*, Vol. 28, 1663–1664, 2003
- [17] T. Tsuchizawa, K. Yamada, H. Fukuda, T. Watanabe, J. Takahashi, M. Takahashi, T. Shoji, E. Tamechika, S. Itabashi, H. Morita, "Microphotonic Devices Based on Silicon Microfabrication Technology", *IEEE Journ. Select. Topics Quant. Electron.*, vol. 11, pp. 232–240, 2005